Configurational Forces in Penetration Processes

Davide Bigoni, Marco Amato and Francesco Dal Corso

Abstract With a loose reference to problems of penetration in biomechanics (for instance, a nanoparticle penetrating through a cell's membrane or a cell sucked with a pipette), the role of configurational forces is investigated during the process in which a compliant intruder is inserted into an elastic structure. For insertion into a rigid constraint, a configurational force proportional to the square of the strain needed to deform the body, which is penetrating, is found. This force has a more complex structure when the compliance of the constraint is kept into account, but in all cases, it tends to expel the penetrating body.

1 Introduction

Biomechanics is a fast developing multidisciplinary science aimed at challenging the secrets of nature. The biomechanics of soft tissues, including successfully modeling of muscles (Stålhand et al. [19]), blood vessels (Holzapfel et al. [14, 15]), brain (Franceschini et al. [13]; Mihai et al. [16]), and vascular tissues (Pandolfi and Holzapfel [17]), is recently oriented to a deeper understanding of the mechanics of the cell (Discher et al. [11]; Boal [5]; Deseri and Zurlo [8]; Terzi et al. [20]; Deseri et al. [9]; Daddi-Moussa-Ider et al. [7]), a field strongly related to several timely problems, including the COVID-19 emergency.

Membrane penetration of nano- or microparticles is a common feature in cell mechanics, important from several points of view, including drug delivery and viral entry. In particular, viral entry into a cell during the early stage of infection may occur in different forms. In the case of penetration, the cell's membrane is punctured after attachment of the virus, which in this way injects its contents inside the cytoplasm.

D. Bigoni, M. Amato and F. Dal Corso
Department of Civil, Environmental and Mechanical Engineering, University of Trento
Via Mesiano 77, I-38123 Trento, Italy
e-mail: bigoni@ing.unitn.it

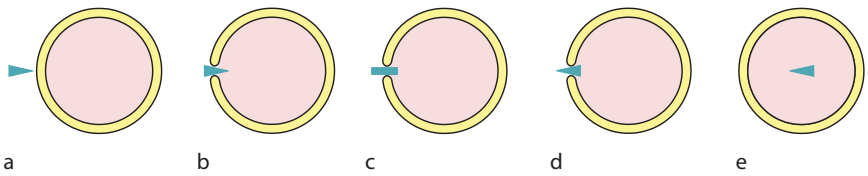

Fig. 1 Schematics of the penetration process: (a) trapping, (b) puncturing, (c) opening, (d) penetration, and (e) end of the process. The penetrating particle and the cell are assumed to be deformable in a two-dimensional formulation, where friction, dissipation, and interparticle non-mechanical interactions are neglected.

Cells may be subject to large deformations, a situation occurring, for instance, when a cell is drawn up a pipette, as is the case of a human red blood cell (Discher et al. [10]). This process involves a competition between forces tending to inject and eject the cell. Similarly, but at a smaller scale, the influenza A virus can be trapped into a nanotube with an internal diameter of 400 nm (Yuge et al. [21]). Membrane penetration and pipette suction are just two examples of problems involving the insertion of a compliant body inside a soft (the membrane) or a rigid (the pipette) structure. Many other problems of this kind can be listed in biomechanics: endoscopy, insertion of a catheter into a blood vessel or into the urinary tract, or injection of a needle for biopsy or for puncturing tissues (Roxhed et al. [18]).

In the present article, the penetration of a compliant body into an elastic structure (such as a cell's membrane) or into a rigid constraint (as when a cell is drawn up a pipette) is analyzed from a purely mechanical perspective, under simple assumptions. These include restriction to the two-dimensional formulation (a gross, but common, approximation (Daddi-Moussa-Ider et al. [7])) and absence of: (i) friction, (ii) dissipative forces, and (iii) interparticle non-mechanical interactions, such as, for instance, magnetic attraction. The simple mechanical process of penetration schematized in Fig. 1 is addressed, with the specific purpose to explore and present the role of configurational forces, actions that develop when an elastic system can change its configuration through a release of elastic energy. These forces have been introduced by Eshelby [12] to describe the mechanics of defects and only recently explored in elastic structures subject to bending (Bigoni et al. [4]) and torsion (Bigoni et al. [3]). Configurational forces in structures lead to unexpected effects, such as possibility of self-encapsulation (Bosi et al. [6]) and expulsion during a penetration process ([2]) due to bending flexibility of inextensible rods.

2 Penetration and Configurational Forces

A simple model is introduced, which may capture essential features of the 'puncturing' and 'penetrating' stages of the intrusion process, shown in Fig. 1. Besides its

application to mechanobiology, the model is formulated to introduce the role of the configurational force in the processes of insertion of an elastic body into another.

A deformable elastic layer is considered of initial height h_0, out-of-plane width b_0, and length for the moment left unspecified. This layer has to be inserted between two rigid planar and frictionless constraints, placed at a distance $\bar{h} \leq h_0$ along the x_2-axis when the two linear elastic springs of stiffness k are unloaded, see Fig. 2(a). These two rigid plates are prescribed to remain parallel to the $x_1 - x_3$ plane.

The spring stiffness k simply models the elastic stiffness of the structure in which the intruder has to penetrate. For instance, when the structure is a thin elastic ring (as sketched in Fig. 1) of radius R and bending stiffness EJ, the spring stiffness becomes $k = 2EJ/(3\pi R^3)$. The elastic layer is partially inserted (of an amount $l > 0$) between the two frictionless constraints so that a deformed configuration such as that illustrated in Fig. 2(b) is realized, where the height of the inserted layer is $h \in \left[\bar{h}, h_0\right]$. Although near the edge of the constraint exit, the stress/strain state is highly disuniform, the unloaded configuration is reached at a sufficient distance far from the constraint's exit, while a state of uniaxial compression is approached inside the rigid plates (where the width of the layer becomes $b \geq b_0$). Therefore, the edges of the constraint induce a strong disturbance, but the stress/strain state tends to become uniform far from this point, when the elastic layer is sufficiently long. Since the contact between the layer and the constraint is smooth, one would be tempted to conclude that no horizontal forces are applied to the elastic body along the x_1-axis. This too facile conclusion is missing the forces which develop at the corners of the constraint, representing the 'microscopic' counterpart of the configurational force concept. In particular, the configurational force can be understood as follows. The total potential energy $\mathcal{V}$ of the deformed system represented in Fig. 2 is coincident

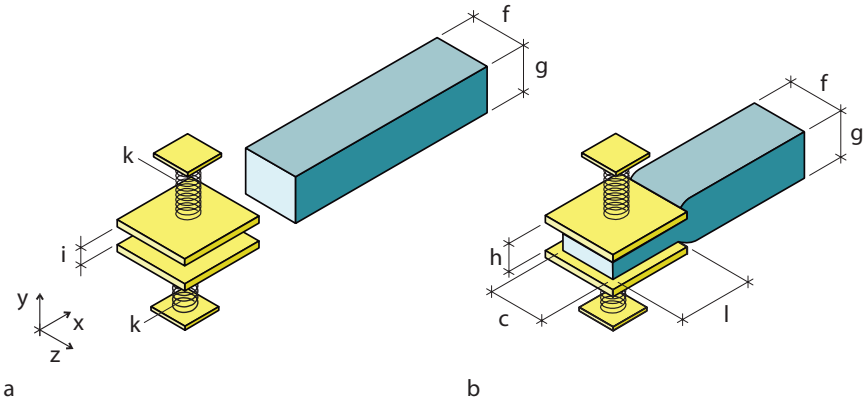

Fig. 2 An elastic layer is inserted between two rigid, flat, and frictionless plates (remaining parallel to the $x_1 - x_3$ plane), each held by a linear spring of elastic stiffness k. The distance between the two rigid plates at rest is $\bar{h}$, smaller than the height h_0 of the elastic layer (a prism of initial cross-section $h_0 \times b_0$) in its unstressed configuration. In the deformed configuration, the prism height is $h \in \left[\bar{h}, h_0\right]$, the width is $b \geq b_0$, and the insertion length is l.

with the elastic energy $\mathcal{E}$, which is given by the sum of that stored in the springs and in the layer. This energy has to depend on the configurational parameter l, i.e. the amount of layer inside the constraint. If l decreases, the energy $\mathcal{V}(l) = \mathcal{E}(l)$ will decrease too, until becoming null when the layer loses contact with the rigid plates because outside ($l \leq 0$). Eshelby [12] defined the configurational force P acting on the elastic system as the negative of the partial derivative of the total potential energy $\mathcal{V}(l)$ at equilibrium with respect to the configurational parameter. In the present case, the configurational force reduces to

$$P = -\frac{\mathrm{d}\mathcal{E}(l)}{\mathrm{d}l}, \tag{1}$$

where the '$-$' sign arises from the fact that on increasing l, the layer moves in the negative direction of the x_1-axis. Therefore, a configurational force emerges, which pushes the layer outside the constraint and can be viewed from a 'microscopic' point of view as the tangential reaction at the frictionless sliding constraint, provided as the resultant of the actions realized at the constraints corners.

The elastic energies stored in the layer and in the springs can be evaluated in an approximate way as follows. The strain-energy density function W for an incompressible Mooney-Rivlin material is (Bigoni [1])

$$W(\lambda_1, \lambda_2, \lambda_3) = \frac{\mu_1}{2}\left(\lambda_1^2 + \lambda_2^2 + \lambda_3^2 - 3\right) - \frac{\mu_2}{2}\left(\frac{1}{\lambda_1^2} + \frac{1}{\lambda_2^2} + \frac{1}{\lambda_3^2} - 3\right), \tag{2}$$

where μ_1 and μ_2 are material constants, while λ_1, λ_2, and λ_3 are the principal stretches, the latter subject to the incompressibility constraint

$$\lambda_1\lambda_2\lambda_3 = 1. \tag{3}$$

The moduli μ_1 and μ_2 are subject to the restrictions

$$\mu_1 \geq 0, \qquad \mu_2 \leq 0, \tag{4}$$

and values representative for the behavior of rubber at room temperature are $\mu_1 = 3\,\mathrm{bar}$ and $\mu_2 = -0.3\,\mathrm{bar}$.

Consider a parallelepiped of initial height h_0 and transverse dimensions l_0 and b_0, compressed parallel to the edge h_0 with a uniaxial state of stress, reducing the height to h and enlarging the other two dimensions to l and b. The stretches are

$$\lambda_1 = \frac{l}{l_0}, \qquad \lambda_2 = \frac{h}{h_0}, \qquad \lambda_3 = \frac{b}{b_0}, \tag{5}$$

which, due to loading symmetry ($\lambda_1 = \lambda_3$) and material incompressibility (eq. (3)), are constrained by

$$\lambda_1 = \frac{l}{l_0} = \lambda_3 = \frac{b}{b_0} = \sqrt{\frac{h_0}{h}}. \tag{6}$$

Therefore, the elastic energy stored in the uniformly deformed parallelepiped corresponds to

$$l_0 b_0 h_0 \, W = l\sqrt{\frac{h}{h_0}}\, b_0 h_0 \left[\frac{\mu_1}{2}\left(\frac{h^2}{h_0^2} + 2\frac{h_0}{h} - 3\right) - \frac{\mu_2}{2}\left(\frac{h_0^2}{h^2} + 2\frac{h}{h_0} - 3\right)\right], \tag{7}$$

where the dependency on the parameter l, crucial in the following calculations, has been evidenced.

When the stretch $\lambda_2 = h/h_0$ is close to 1, the energy (eq. (7)) can be approximated by

$$l_0 b_0 h_0 \, W = \frac{3}{2}(\mu_1 - \mu_2)\, l\, b_0\, h_0 \epsilon^2, \tag{8}$$

where ϵ is the infinitesimal strain along the x_2-axis

$$\epsilon = \frac{h}{h_0} - 1, \tag{9}$$

and for small strain, the elastic energy (eq. (7)) reduces for $\mu_1 = \mu$ and $\mu_2 = 0$ to the strain energy of an isotropic and incompressible linear elastic solid.

The energy, as given in eq. (7), provides a simple approximation to that stored in the whole deformed elastic layer. The contribution of the highly inhomogeneous zone near the edge of the constraint is completely neglected, but this approximation becomes reasonable when the parts of the layer inside the constraint and outside are sufficiently long. In this way, the variation of the stored energy when a part of the layer is expelled from the constraint corresponds with a good approximation to the final segment of the layer inside the constraint, which is subject to a stress/strain state approximately uniform and corresponding to uniaxial stress.

2.1 Penetration of a Rigid Body

If the penetrated body in which the elastic intruder is inserted is rigid, $k \to \infty$, the height $h = \bar{h}$ is fixed, and no energy is stored within the springs. In these conditions and for the above considerations, the configurational force P can be easily obtained through differentiation of eq. (7) with respect to the parameter l, i.e.

$$\frac{P}{\mu_1 b_0 h_0} = -\frac{1}{2}\sqrt{\frac{h}{h_0}}\left[\frac{h^2}{h_0^2} + 2\frac{h_0}{h} - 3 - \frac{\mu_2}{\mu_1}\left(\frac{h_0^2}{h^2} + 2\frac{h}{h_0} - 3\right)\right]. \tag{10}$$

Using the conditions stated in eq. (4), it can be seen from eq. (10) that the configurational force is negative ($P < 0$), and therefore, it tends to expel the layer from the constraint (in other words, to move it in the positive direction of the x_1-axis).

Equation (10) is a complex function of the elastic energy via the stretch $\lambda_2 = h/h_0$ and shows the independence of the length l for the configurational force P. When

the strain ϵ is small, the configurational force P can be approximated as a quadratic expression of the infinitesimal strain ϵ, i.e.

$$\frac{P}{\mu_1 b_0 h_0} = -\frac{3}{2}\left(1 - \frac{\mu_2}{\mu_1}\right)\epsilon^2. \tag{11}$$

2.2 Role of Penetrated Body's Elasticity

In this section, the effect of the elasticity of the structure penetrated by the intruding layer is accounted for by considering each rigid plate suspended by a linear elastic spring of stiffness k, as illustrated in Fig. 2. The total elastic energy $\mathcal{E}$, consisting of the energies stored in the two springs of stiffness k and the elastic layer, is

$$\frac{\mathcal{E}}{\mu_1 b_0 h_0} = \frac{k h_0}{4\mu_1 b_0}\left(\frac{h}{h_0} - \frac{\bar{h}}{h_0}\right)^2 + \frac{l}{2}\sqrt{\frac{h}{h_0}}\left[\frac{h^2}{h_0^2} + 2\frac{h_0}{h} - 3 - \frac{\mu_2}{\mu_1}\left(\frac{h_0^2}{h^2} + 2\frac{h}{h_0} - 3\right)\right]. \tag{12}$$

In this case, the height h is not imposed, as in eq. (10), but is an unknown, which depends on the relative stiffness between the springs and the elastic layer. To proceed further, the small strain assumption is introduced, together with $\mu_1 = \mu$ and $\mu_2 = 0$. Under these restrictions, the configurational force can be easily calculated as follows. The total elastic energy $\mathcal{E}$ (eq. (12)) becomes a function of the (small) strain ϵ in the layer and reads

$$\frac{\mathcal{E}(\epsilon, l)}{\mu b_0 h_0} = \frac{k h_0}{4\mu b_0}\left(1 + \epsilon - \frac{\bar{h}}{h_0}\right)^2 + \frac{3}{2} l \epsilon^2. \tag{13}$$

The stationarity of the total energy $\mathcal{E}(\epsilon, l)$, as introduced in eq. (13), with varying the strain ϵ in the layer gives the strain ϵ^* at equilibrium for a given length l, i.e.

$$\epsilon^*(l) = -\frac{1 - \dfrac{\bar{h}}{h_0}}{1 + \dfrac{6\mu b_0 l}{k h_0}} \tag{14}$$

(a negative quantity because of $\bar{h}/h_0 < 1$). Hence, the total elastic energy (eq. (13)) evaluated at ϵ^* is

$$\frac{\mathcal{E}(\epsilon^*(l), l)}{\mu b_0 h_0} = \frac{k h_0}{4\mu b_0}\frac{\left(1 - \dfrac{\bar{h}}{h_0}\right)^2}{1 + \dfrac{k h_0}{6\mu b_0 l}}. \tag{15}$$

Using eq. (1), the configurational force P reads

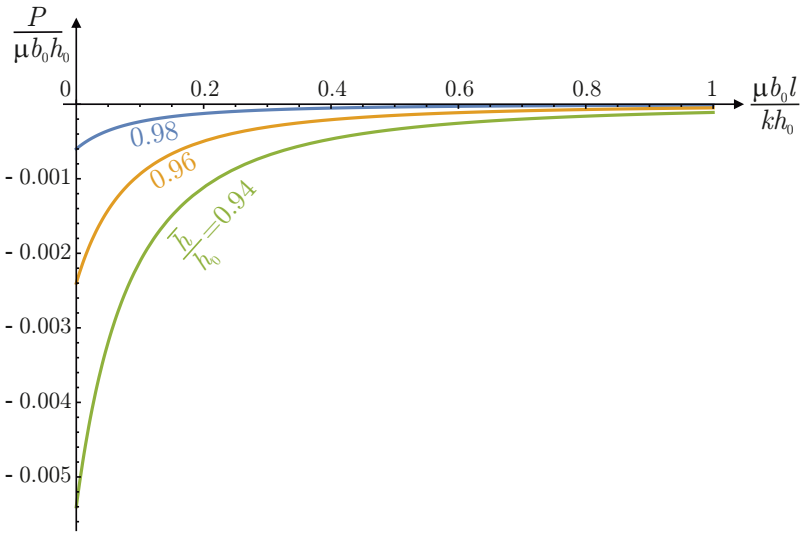

Fig. 3 Configurational force P, made dimensionless through division by $\mu b_0 h_0$, as a function of $\mu b_0 l/(k h_0)$ for three values of the ratio $\bar{h}/h_0 = \{0.94, 0.96, 0.98\}$.

$$\frac{P}{\mu b_0 h_0} = -\frac{3}{2}\left(\frac{1-\dfrac{\bar{h}}{h_0}}{1+\dfrac{6\mu b_0 l}{k h_0}}\right)^2 \tag{16}$$

and is reported in Fig. 3 as a function of $\mu b_0 l/(k h_0)$, for three values of the ratio $\bar{h}/h_0$, chosen close to one. At vanishing $\mu b_0 l/(k h_0)$, a finite limit is attained for the force P, i.e.

$$\lim_{\frac{\mu b_0 l}{k h_0}\to 0} \frac{P}{\mu b_0 h_0} = -\frac{3}{2}\left(1-\frac{\bar{h}}{h_0}\right)^2, \tag{17}$$

which corresponds to the value obtained under the approximation that the penetrated body is rigid (see Eq. (11)), by identifying the distance $\bar{h}$ between the rigid plates at rest with h.

3 Conclusion

Penetration of one body into another is a common process in biomechanics. It has been shown in the present note that configurational forces may play an important role in these processes. The configurational forces can be calculated by considering the stored elastic energy and represent the counterpart of the microscopic actions

developing at the moving boundary points, present at the contact between the intruder and the penetrated body.

Acknowledgments. Financial support is acknowledged from H2020-MSCA-ITN-2020-LIGHTEN-956547 and ARS01-01384-PROSCAN.

References

1. Bigoni, D.: Nonlinear Solid Mechanics: Bifurcation Theory and Material Instability. Cambridge University Press (2012)
2. Bigoni, D., Bosi, F., Dal Corso, F., Misseroni, D.: Instability of a penetrating blade. J. Mech. Phys. Solids **64**, 411–425 (2014)
3. Bigoni, D., Dal Corso, F., Misseroni, D., Bosi, F.: Torsional locomotion. Proc. Math. Phys. Eng. Sci. **470**, 20140599 (2014)
4. Bigoni, D., Dal Corso, F., Bosi, F., Misseroni, D.: Eshelby-like forces acting on elastic structures: theoretical and experimental proof. Mech. Mater. **80**, 368–374 (2015)
5. Boal, D.: Mechanics of the Cell. Cambridge University Press, Cambridge (2002)
6. Bosi, F., Misseroni, D., Dal Corso, F., Bigoni, D.: Self-encapsulation, or the 'dripping' of an elastic rod. Proc. Math. Phys. Eng. Sci. **471**, 20150195 (2015)
7. Daddi-Moussa-Ider, A., Goh, S., Liebchen, B., Hoell, C., Mathijssen, A.J., Guzmán-Lastra, F., Scholz, C., Menzel, A.M., Löwen, H.: Membrane penetration and trapping of an active particle. J. Chem. Phys. **150**, 064906 (2019)
8. Deseri, L., Zurlo, G.: The stretching elasticity of biomembranes determines their line tension and bending rigidity. Biomech. Model. Mechanobiol. **12**, 1233–1242 (2013)
9. Deseri, L., Pollaci, P., Zingales, M., Dayal, K.: Fractional hereditariness of lipid membranes: Instabilities and linearized evolution. J. Mech. Behav. Biomed. Mater. **58**, 11–27 (2016)
10. Discher, D., Mohandas, N., Evans, E.: Molecular maps of red cell deformation: hidden elasticity and in situ connectivity. Science **266**, 1032–1035 (1994)
11. Discher, D.E., Boal, D.H., Boey, S.K.: Simulations of the erythrocyte cytoskeleton at large deformation. II. Micropipette aspiration. Biophys. J. **75**, 1584–1597 (1998)
12. Eshelby, J.D.: The force on an elastic singularity. Philos. Trans. Royal Soc. A **244**, 87–112 (1951)
13. Franceschini, G., Bigoni, D., Regitnig, P., Holzapfel, G.A.: Brain tissue deforms similarly to filled elastomers and follows consolidation theory. J. Mech. Phys. Solids **54**, 2592–2620 (2006)
14. Holzapfel, G.A., Gasser, T.C., Ogden, R.W.: A new constitutive framework for arterial wall mechanics and a comparative study of material models. J. Elasticity **61**, 1–48 (2000)

15. Holzapfel, G.A., Sommer, G., Regitnig, P.: Anisotropic mechanical properties of tissue components in human atherosclerotic plaques. J. Biomech. Eng. **126**, 657–665 (2004)
16. Mihai, L.A., Budday, S., Holzapfel, G.A., Kuhl, E., Goriely, A.: A family of hyperelastic models for human brain tissue. J. Mech. Phys. Solids **106**, 60–79 (2017)
17. Pandolfi, A., Holzapfel, G.A.: Three-dimensional modeling and computational analysis of the human cornea considering distributed collagen fibril orientations. J. Biomech. Eng. **130**, 061006 (2008)
18. Roxhed, N., Gasser, T.C., Griss, P., Holzapfel, G.A., Stemme, G.: Penetration-enhanced ultrasharp microneedles and prediction on skin interaction for efficient transdermal drug delivery. IEEE J. Microelectromech. Syst. **16**, 1429–1440 (2007)
19. Stålhand, J., Klarbring, A., Holzapfel, G.A.: Smooth muscle contraction: mechanochemical formulation for homogeneous finite strains. Prog. Biophys. Mol. Biol. **96**, 465–481 (2008)
20. Terzi, M.M., Dayal, K., Deseri, L., Deserno, M.: Revisiting the link between lipid membrane elasticity and microscopic continuum models. Biophys. J. **108**, 87a–88a (2015)
21. Yuge, S., Akiyama, M., Ishii, M., Namkoong, H., Yagi, K., Nakai, Y., Adachi, R., Komatsu, T.: Glycoprotein nanotube traps influenza virus. Chem. Lett. **46**, 95–97 (2017)